

DC Microgrid Subsystems in AC Network Fault Detection and Localization Using Artificial Intelligence: A Review

Zukisa Nante^{*,†}, Zenghui Wang[†]

Department of Electrical and Smart Systems Engineering, University of South Africa, Florida 1709, South Africa

Abstract

A major challenge of a microgrid (MG) system is to design its protection system. The protection system response should be for utility network system and MG faults. Faults viz., (1) value changes and monitoring if the connection is established or not for the overcurrent path conditioned upon a distributed generator (DG), (2) decreased detecting ability drawn on Distributed Energy Resource (DER) networks, (3) unintentionally power cuts caused by faults from the neighboring lines because of DER participation, (4) line reconnection by a breaker linking two points with or without delay during fault occurrence and fuse failure during transient faults, and (5) closed circuit and local area network topology using DER. Increasing demand of electricity has led to the growth in adoption of electrical MGs in electrical distribution systems, thus, this paper reviews the utilization of Machine learning (ML) methods in direct current (DC) subsystems in a alternating current (AC) network on detecting and localizing faults. These MG challenges impact the consistency and steadiness in power systems; hence, reviewing ML methods for fault detection and localization is critical. In literature ML methods are used individually or combined (hybrid) for fault detection and localization and discusses and reviews the possible combination of Principal Component Analysis (PCA), K-means clustering, Convolutional Neural Networks (CNN), Genetic Algorithm (GA), and eXplainable Artificial Intelligence (XAI) to detect, localize, and explain faults. Nevertheless, this paper will not review all the methods of machine learning, but the ones mentioned above.

Keywords

Fault Detection, Fault Localization, Fault Classification, Microgrid, Neural Networks

1. Introduction

Over the years, the development of renewable energy rose to address the global problems, namely, increasing energy demand, environmental issues, and fossil fuel exhaustion. This led to MGs development allowing more distributed energy resources connected with power grids [1]. Grid development should conform consistency, lessen carbon emanation and reduce costs. It consists of transmission lines, and with a single transmission line consisting specified distance sharing self-same voltage and current. They accurately and reliably conduct electrical

The 6th International Symposium on Advanced Technologies and Applications in the Internet of Things (ATAIT 2024), August 19-22, 2024, Kusatsu, Shiga, Japan

*Corresponding author.


[†]These authors contributed equally.

✉ 37229958@mylife.unisa.ac.za (Z. Nante); wangz@unisa.ac.za (Z. Wang)

ORCID 0009-0005-5968-5782 (Z. Nante); 0000-0003-3025-336x (Z. Wang)

© 2024 Copyright for this paper by its authors.

Use permitted under Creative Commons License Attribution 4.0 International (CC BY 4.0).

 CEUR Workshop Proceedings (CEUR-WS.org)

energy. However, collateral arrangements, with mutual coupling effects make protection a challenge. Detecting and locating faults in power system operations need crucial methods to ensure defensiveness, reliability, and self-repair. Effectively, fault detection gives fault isolation protective relays good operability and cuts power from faulty grid portion. Therefore, fault detection and localization provided a fault occurs answer the questions like: what type of fault is detected and where is it located? Faults should be properly designed to avoid severe components damages and costly interruption. Thus, this research focuses on fault detection and localization problems in MGs. Fault detection process identifies the anomalies, while fault localization process determines the position of the fault.

A fault can be seen or defined as an irregular electric current that travels in an unintended path due to contacts between live wire and short-to-ground, or caused by faulty apparatus viz., convertors, men mistakes and environmental changes. Other possible faults could be due to open circuit, high resistance, and short-to-power. The voltage and current level alter during fault occurrence in the utility structure [2]. Thus, locating faults is very handy in lengthy connections and in challenging areas where inspection is problematic to conduct and unbearable. In such situations, eXplainable Artificial Intelligence (XAI) can play a big role in explaining the fault type to technical staff [3]. The idea behind XAI is to provide human-understandable explanations to the decisions made by the classification algorithm. These are the decisions generated by AI and the ML models. These models are divided into two categories: model-specific methods and model-agnostic methods. Model-specific methods scope is limited and can be applied to linear regression, decision trees, and neural network interpretability. As opposed to model-specific methods, model-agnostic methods can be applied to any ML model, regardless of the type or structure. Model-agnostic method focuses on data analyzation of the input-output feature pairs. This method incorporates AI systems such as Local Interpretable Model-agnostic Explanations (LIME) and SHapley Additive exPlanations (SHAP) to manifest model interpretability certainty. LIME explains the predictions of the model individual cases rather than the whole model dataset predictions. SHAP on the other hand, explains by calculating individual feature contribution per case. Visual inspection is also difficult during bad weather conditions.

Hence, locating faults is crucial and automatic fault detection is beneficiary for the MG system's reliability. For fault detection, parameters like voltage and current alteration, pre and post fault frequency signals are measured. Power plant controller (PCC) controls faults via a static switch, to isolate a MG and main grid when fault occurs. [4] proposed a fault identification approach under MG different situations and enabled a backing protector for intelligent MGs DERs of excessive penetration. Fault detection based on initiating failures and clearing the intervals responsible for the noise magnitude, and DERs effect on grid networks and isolated MGs. Fault localization and isolation based on supervised learning for centralized fault localization. Backup protection using two phasor measurement units (PMUs) on the distribution feeder to help empower the microgrid central protection unit (MCPU) carrying out remedial actions in case of relay malfunctioning. And finally, prevent unstable operation of DERs. [5] proposed a technique that estimates the direction of the fault by using Negative Sequence Superimposed Impedance Angle (NSSIA) magnitude. It performed well on various uncertainties of DG generation and frequencies.

[6] proposed a solution to the fault detection and fault localization problem by utilizing three techniques viz., Decision Tree (DT), Random Forest (RF) and neural network (NN). RF obtained

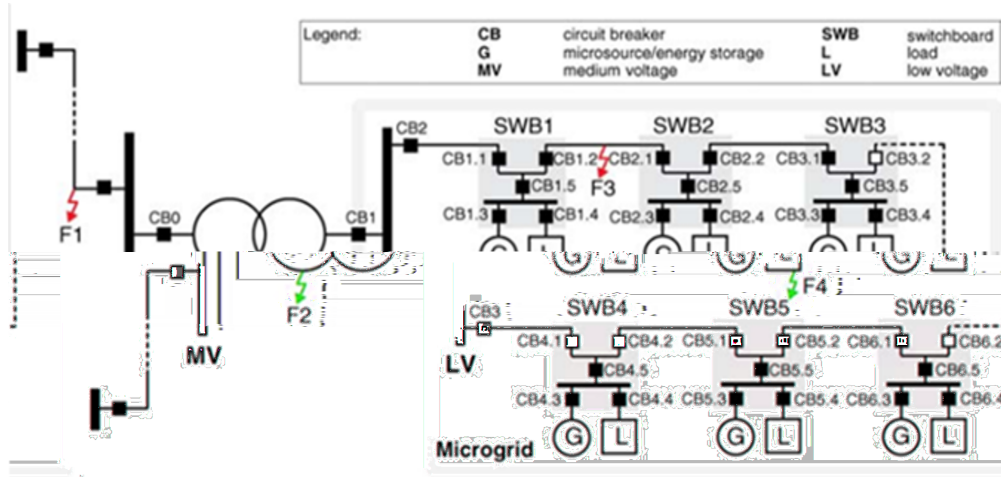


Figure 1: Outside and inside faults of MGs.

an accuracy of 99% for fault prediction. The focus was on predicting the fault type, faulty cable and lastly detecting total length from the distribution system. The dataset was generated using MATLAB simulations and each fault was sustained for 5 seconds. The Root Mean Square (RMS) value of the three phase voltages and currents signals at three sources are collected. Burdens viz., line-line-line (LLL) fault, line-line-line-ground (LLLG) fault, single line to ground fault (LG), line-line (LL) fault or line-line-ground (LLG) created a bigger dataset. From tests NN didn't perform well due to poor precision and longer execution time. Though obtained better results with the RF, there is still a gap as CNN can perform better than artificial neural network (ANN) for image recognition (voltage and current data converted into images). Therefore, the same dataset can be transformed into images and utilized as CNN input and only manipulate the parameters to enhance training time and accuracy. To overcome the longer execution time, PCA can be used for data dimensionality reduction in a big dataset while maintaining important features to enhance the training or execution time. The paper organization structure: Section I introduction, Section II MG theoretical background and protection zones, Section III MG challenges review, Section IV ML methods, and Section V conclusion.

2. MG theoretical background and protection zones

Figure 1 represents outside and inside faults in a distribution system (MG included) with local network protective zones such as overhead cables, and lines such as buses, transformers, generators, and loads. A distribution protection system contains basic design criteria viz., sensitivity, selectivity, and speed; and they are abbreviated as "3S". Whereby, sensitivity states that the protection system should identify an abnormal disorder that surpasses the normal threshold value. Selectivity represents the system's ability to disconnect the faulted part only and minimize fault consequences. Finally, the speed that the protective relays should have to react to unusual situations within feasible time avoiding equipment harm and maintaining system steadiness.

From Figure 1 the following faults F1, F2, F3 and F4 are discussed.

F1 is detached through circuit breaker (CB)1 within 70 ms dependent on the voltage sag level in the MG. CB1 detaches MG from the master network when protection via medium voltage (MV) fails to trip. However, detecting F1 through overcurrent relay could be challenging due to DERs linked through power electronics (PE) components integrated with fault current constraint. Hence, the answer is to utilize directional overcurrent relay in CB1 provided current usage is for detecting faults; and consider DERs representing subdivided elements contributing to the short-circuit current on the specified direction. The output current is calculated by using (1) whereby I_{rDER} represents DER output current and K_{DER} the fault current 1.1 factor aimed at PE liaised DER and at 5.0 aimed at concurrent DER elements.

$$I_{kmin} = \sum_{1}^n K_{DER} * I_{rDER}, \quad (1)$$

For F2 fault, the supply transformer overcurrent (OC) protection opens CB0 to remove faulty line, and CB1 opens at the same time via a “follow-me” function of CB0. However, hardware lock failure is a conceivable fault issue. A possible solution is the utilization of directional adaptive OC defense, below-voltage and below-frequency safeguard including different islanding detection techniques. For F3 fault, MG CB1.2 and CB2.1 detach the potential portion of the low voltage (LV) feeder. High short-circuit current distributed by the main MV grid opens CB1.2. If CB1.2 fails to trip, CB1.1 (CB1.2 backup) removes F3 faults. However, CB1.1 protection relay could be disturbed provided a substantial synchronous DER installation has taken place and turned on at switchboard 1 (SWB1). Hence, a solution to this is bringing together MG and DER protection systems and modifying the protection settings of current operating conditions (DER status). Fault F4 occurs at the end-consumer site in grid connected mode and it is caused by a high short-circuit current provided to F4 fault via master net, and DER role tripping CB2.4. A fuse is used instead of a CB and if set off occurred, SWB2 detachment is via CB2.5 and local DER is removed. Fault computations are common in electrical systems computations conducted throughout the analysis and design phase and these computations aid to establish the current in circuit elements in irregular situations like short circuits and earth faults. Electrical fault types are transient faults, asymmetric faults, and symmetric or balanced faults. The focus of this study will look more into asymmetric faults which are line-to-line, line-to-ground, and double line-to-ground faults. A transient fault refers to the absence of fault when shortly detaching power and later reinstated. It briefly impacts a device’s insulation, but later reinstated. They can be caused by transient tree contactors or birds. Symmetrical faults or balanced faults are three-phase faults, whereby all three phases short-circuit to the ground or together, and these are faults that give rise to symmetrical fault currents. They may hugely harm appliances yet still operationally balanced. CBs, set-phase relay, and other protective switchgear help for their analysis per phase based on bus impedance matrix or Thevenin’s theorem. Thevenin’s theorem states that, any linear electrical network containing only voltage sources, current sources and resistances can be replaced at terminals A–B by an equivalent combination of a voltage source V_{th} in a series connection with a resistance R_{th} . For a three-phase: any three-terminal active linear network can be substituted by three voltage sources with corresponding impedances, connected in wye or in delta.

$$V_{Th} = \frac{R_2 + R_3}{(R_2 + R_3) + R_4} \cdot V_1, \quad (2)$$

An asymmetric or unbalanced fault is a line-to-line (L-L) or phase-to-phase (P-P) fault that affects phases unequally. It is short circuited among branches, air ionized, or lines (cables) physical contact occurrence. Transmission cable faults occur about 5% -10%. Another asymmetric fault type to look at is a double line-to-ground or two-phase-to-earth fault (L-L-G) that happens during two-line contact plus the ground through storms and in transmission cable faults this occurs about 15% - 20%.

3. MG challenges overview

3.1. MG challenges

One of the most critical concerns in MG is a well-defined protection scheme [7]. MGs challenges such as the demand changes, export limits, generation, and short circuit fault currents require an appropriate protection strategy that will ensure the system meets its demands. Direct Current (DC) MGs parts like convertors get damaged by high fault current. Hence, a convertor loses control over voltage and current because they demand high power ranking that raises expenses, and surges additional protection areas. Due to these challenges fault detection and localization are critical. Currently, many state-of-the-art theorems or techniques namely, (1) signal processing based methods: wavelet transform (WT), fast Fourier transform (FFT), short time Fourier transform (STFT), s-transform (Gabor and wavelet transforms), background noise, Hilbert-Huang transform, and mathematical morphology; and (2) advanced methods: fuzzy logic, deep neural network (DNN), ANN, and decision tree-based developed by researchers, academics, private and governmental institutions seeking to address faults in AC/DC MGs, [8].

This paper aims to review and peruse the ML current techniques for fault detection and localization in DC subsystems in a AC network. [9] points out the DERs malfunctioning exacerbation in MGs islanded protection systems including limitation challenges possessed by typical protection systems. Protection systems viz., overcurrent relaying, facing novel complications, protection blinding, sympathetic set off, and backup catastrophe. Also, DERs connections altering the short-circuit currents value and route; commencing from the upstream network affecting upstream protective devices fast response and even the failing of the relays on detecting fault occurrence. When utilizing the DERs it can be expected that they may cause organizational issues as typical relays might experience fault detection delays. Hence, delaying circuit breakers (CBs) may affect postfault voltage steadiness of MGs, and worse that may cause series failures[10]. Thus, DERs penetrating levels and uncertainties affect a protective device's fault detection capability when faults occur. It is therefore significant to have a fault detection and localization method that can quickly detect, classify, and localize faults. Moreover, visually depicts and explains these faults to field technical staff. ML methods such as CNNs, PCA, K-means, GA, and XAI worth to be studied as they offer better classification, speed, accuracy, and understanding. PCA helps with dimensional reduction. K-Means clustering may help identify the similarities between the data instances. While CNNs are proficient in classifying images (data format) fast and accurate; and in this case, images will be the converted fault,

training, and validation data. Though, there exist hybrid algorithms to solve the fault detection and localization problem, currently, there is no proposed hybrid of PCA, K-means, CNN, GA, and XAI found in literature. In this study, fault detection and localization optimization challenge is reviewed.

4. ML methods

4.1. PCA

PCA is an interesting unsupervised algorithm that can be utilized for dimensionality reduction and feature extraction converting data toward new feature area expecting it will maintain useful features. Dimensionality reduction enhances the required memory computation to train fast. However, this research interprets it as a supervised method for fault location.

Assuming that the fault location is determined by similar high-frequency transients; taking the highs and lows from the fault transients and denote them as attribute nodes and analyzing signal after fault to classify attribute nodes via window-based local maxima or minima technique. Attribute nodes such as intermediate sample distances ($\Delta\tau$) depending on fault location (D) parameter are calculated as fault resistance (R) and fault inception angle or FIA ($\Delta\Phi$) parameters will not affect the ($\Delta\tau$) values. Therefore, PCA generates principal directions of variations and eliminates the minor parametric disturbances of ($\Delta\tau$) values. Because PCA feature extracts multivariate data using principal components (PCs), these PCs can help show pathways of maximum changes in downward ranking order.

Supposing that the regularized data are $X = [x_1, x_2, \dots, x_n]^T \in R^{n \times m}$, the equation includes n variables and m samples. Deriving PCA objective function we need a projection vector \vec{p} , with $y_i = \vec{p}^T x_i$, and therefore, PCA objection function is:

$$J_{PCA}(\vec{p}) = \max \left(\frac{1}{n} \sum_i^n (y_i)(y_i)^T \right), \quad (3)$$

where $\vec{p}^T \vec{p} = 1$, and in that case (4) and (5) demonstrate this:

$$X = T\vec{P}^T + E, \quad (4)$$

$$C = \frac{1}{n} X X^T, \quad (5)$$

Where X represents regularized data, and $P \in R^{m \times k}$ representing loading matrix. By eigen decomposition of C , we can get $T^{n \times k}$ which determines score matrix, and E as residual matrix. Here, k , is PCs quantity and its computation is achieved via increasing variance influence rate as follows:

$$\sum_{i=1}^n \lambda_i / \sum_{i=1}^n \lambda_i \times 100\% \geq \sigma, \quad (6)$$

Whereby λ_i signifies eigenvalue of the C eigenvalue breakdown with the larger to petite arrangement. σ representing maximum eigenvalues sum relationship in eigenvalues, and normally summing to 85%. With the knowledge that fault diagnosis only checks if a fault has occurred or not, we can then say it uses two statistics of T^2 and Q to validate fault occurrence. Here T^2 statistic represents Hotelling's T-squared distribution suggested by (Hotelling, 1931)¹ and its purpose is to reflect spatial characteristics differences for PCs and can be expressed as follows:

$$T^2 = x_i^T P S^{-1} x_i, \quad (7)$$

While on the other hand the Q -statistic acknowledged as Squared Prediction Error Index (SPE) echoes subspace characteristics differences of the residuals described as follows:

$$\text{SPE} = e^T e, \quad (8)$$

Therefore, T^2 controller restrictions and Q statistics are D_C and $Q_{C,\alpha}$ correspondingly. Both these control limits can be formulated as follows:

$$D_C = \frac{l(n^2 - 1)}{n(n - 1)} F_\alpha(l, n - l), \quad (9)$$

$$Q_{C,\alpha} = \theta_1 - \theta_2 h_0 \left(\frac{1 - h_0}{\theta_1^2} \right) + \frac{\sqrt{z_\alpha (2\theta_2 h_0^2)}}{\theta_1}, \quad (10)$$

where...

$$\theta_i = \sum_{j=l+1}^m \lambda_j^i (i = 1, 2, 3), \quad (11)$$

and

$$h_0 = 1 - \frac{2\theta_1\theta_3}{3\theta_2^2}, \quad (12)$$

respectively. With n representing the modelled data samples quantity, l the PCs retained quantity, α the significance level, F the distribution critical value under $l, n-1$ in the statistical table, C_α ordinary supply critical value at consequential altitude α , and finally λ_i representing smaller eigenvalue of data covariance matrix.

4.2. GA method

One of the features of the RTA system is that a task should be executed within a particular time constraint, therefore, RTA is critical for line fault location. Hence, utilizing an algorithm that is fast and can quickly locate faults is important. Because GA is a multi-objective optimization algorithm it seems logic to use it to locate faults fast. According to [11] GA utilization helps

¹Hotelling, H. (1931). The Generalization of Student's Ratio. Springer eBooks, pp.54-65. doi: https://doi.org/10.1007/978-1-4612-0919-5_4

on the fault line parameters identification and uses these line parameters on finding the fault location. Also, noted during simulations that this algorithm can diagnose a fault just in 1ms time and its maximum error fault location is 0.5%. One of its advantages is that fault location has no impact on fault diagnosis. Figure 2 depicts a DC MG system:

Categorized faults into three stages such as, (1) DC side capacitor discharge stage; (2) diode continuation stage; and (3) AC side provides current favouring DC part voltage recuperation settling for stable status phase. Because the focus on this research was more on detecting faults from the converter and in the line, their first assumption was that if a fault happens between Node 1 and Node 2, it is best to strip down the converter and peruse the functional circuit diagram by analysing the characteristics of the capacitive emancipation stage fault namely: (1) capacitive emancipation stage characteristic examination through ordinary system task; (2) capacitive emancipation stage distinctive analysis through single pole ground fault; (3) capacitive emancipation stage distinctive investigation through inter-pole short circuit fault. Therefore, during the positive grounding fault occurrence among nodes one and two line, the converter one side comparable circuit diagram is depicted in Figure 3. Whereby, L and R represents the induction and defiance branch amongst line's first end and faulty node. C

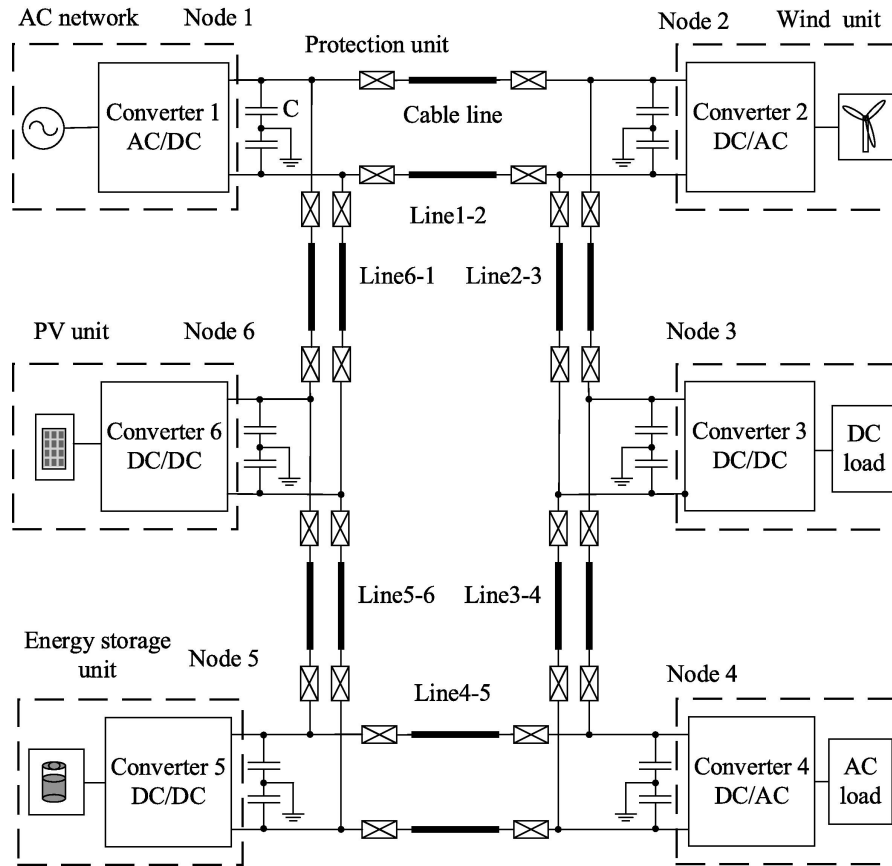


Figure 2: Constructed illustration of DC MG system [11].

represents the one pole capacitance of DC side. R_f , the fault resistance. L_s and $i_{\alpha sabc}$, the three-phase inductance and inductance current of the AC side. i_c , the DC side discharge current of first stage. i_D , continuous diode current in next stage and finally, i_s , current from the AC side to the adjacent DC voltage regaining in the third stage. When again two nodes 1 and 2 inter-pole, short circuit fault occurs. The difference between the unipolar ground fault, and inter-pole short-circuit is the diode renewal phase that equates to a three-phase short-circuit of the AC side.

The method used to diagnose faults was derived from four scenarios viz. positive pole line grounded, positive ground fault at the converter interface, short circuit between line poles, and inter-pole short circuit at the converter. But to be able to analyse and classify faults a DC power distribution side is chosen for DC MG and Figure 4 depicts this. Where C_i represents the positive and negative node i capacitance. C_j , the positive and negative node j side capacitance. $i_p C_i$, $i_n C_i$ and $i_p C_j$, $i_n C_j$ the positive and negative capacitance currents parallel with the converters i and j . Lastly, i_{pi-j} , i_{ni-j} , and i_{pj-i} , i_{nj-i} representing the positive and negative protection installation line currents between converter i and j . Computing the current change rate between 20 - 100 μ s sample time intervals (13) is used:

$$\frac{di}{dt} = \frac{i(k+1) - i(k)}{\Delta t}, \quad (13)$$

Where Δt represents the sampling time interval, k , the sampling constant, $i(k)$ and $i(k+1)$, the current moment sampling value, and the next moment sampling value of the positive and negative line terminal currents respectively. A $1 \times 10^4 \frac{A}{s}$ threshold value ε usage is fault detection occurrence through monitoring the current change rate from both the positive and negative ends of the ε . To stop fault resistance effectiveness the circuit parameters formula for positive ground fault was derived from Kirchhoff's law voltage.

$$u_{dci} = i_i R_i + L_i \frac{di_i}{dt} + (i_i + i_j) R_f, \quad (14)$$

$$u_{dcj} = i_j R_j + L_j \frac{di_j}{dt} + (i_i + i_j) R_f, \quad (15)$$

Therefore, combining (14) and (15)

$$i_j R_j + L_j \frac{di_j}{dt} - i_i R_i - L_i \frac{di_i}{dt} - u_{dci} + u_{dcj} = 0, \quad (16)$$

GA is a developmental technique, meaning a meta heuristic optimization technique applying evolutionary ideologies on solving a problem. Therefore, in solving the problem of fault location we can use the variables or fault line parameters to arrive in a solution. GA feature selection criteria will increase the speed on obtaining the optimal solution by only applying few steps such as, population initialization, fitness calculation, generator operator setting, and finally updating the iterations.

To initialize the population, the genetic coding should exist prior to any production of an individual and this affects crossover and mutation operators. Assuming that the feature retention and loss are a zero-one (0-1) drawback, and that administered data are $X = [x_1, x_2, \dots, x_n]$

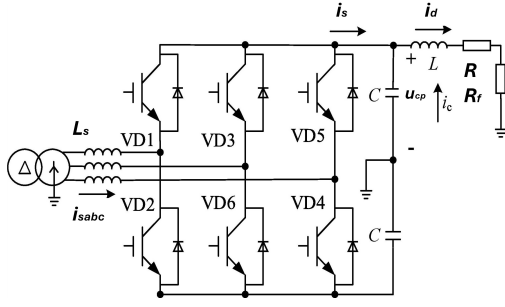


Figure 3: Comparable circuit [10].

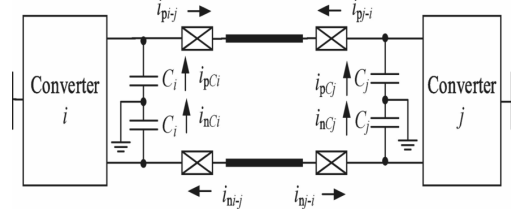


Figure 4: Double-ended DC power supply system [10].

whereby x_n represents attribute data. Thus, provided one meant eigenvector preservation, zero indicates removing that eigenvector; the whole individual genotype represents binary encoded symbol string. From this point we can determine the intensity for each utilizing the fitness function to evaluate the strong and weak individuals.

Therefore, from the processed data $X_1 = [x_1, x_2, \dots, x_m]$, the individual residual space data is $X_2 = [x_1, x_2, \dots, x_k]$, $k + m = n$. Provided data are grouped into two, then, $A = \{a_{-1}, a_{-2}, \dots, a_{-N}\}$, $B = \{b_{-1}, b_{-2}, \dots, b_{-N}\}$, and from this data the Pearson correlation coefficient is defined as follows:

$$\rho_{AB} = \frac{\text{Cov}(A, B)}{\sigma_A \sigma_B} = \frac{\sum_{i=1}^n \frac{(A_i - E(A))}{\sigma_A} \frac{(B_i - E(B))}{\sigma_B}}{n}, \quad (17)$$

$$\therefore \sigma_A = \sqrt{\frac{\sum_{i=1}^n (A_i - E(A))^2}{n + \varepsilon}}, \sigma_B = \sqrt{\frac{\sum_{i=1}^n (B_i - E(B))^2}{n + \varepsilon}}, \quad (18)$$

where ε is a small positive constant and does not affect the value of the n but prevents the denominator from being zero, σ_A , σ_B are the standard deviations of A,B respectively; and $|\rho_{AB}| \leq 1$ is acceptable. From the Pearson correlation coefficients data, we can determine the fitness function:

$$f_{Fit} = \left(p \sum_{i=1}^m \sum_{j=1}^m |\rho_{X_1(i)X_2(j)}| \right) / \left(\sum_{i=1}^{m-1} i \right) + \left((1-p) \sum_{i=1}^m \sum_{j=1}^m |\rho_{X_1(i)X_2(j)}| \right), \quad (19)$$

where $i = 1, 2, \dots, m$ and $j = 1, 2, \dots, k$, f_{Fit} the fitness function, and p the fitness proportion of the two indicators, $0 \leq p \leq 1$.

4.3. K-means

[12], defines k-means as information cluster that joints huge data sets into reduced groups sets of alike information and a technique that preserves good quality features. Mathematically this algorithm is presented as follows:

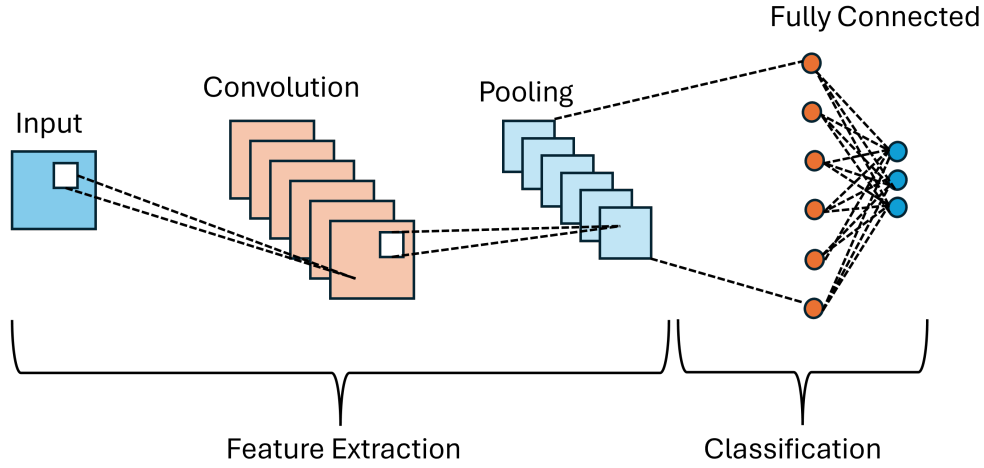


Figure 5: CNN architecture [13].

$$J = \sum_{j=1}^k \cdot \sum_{i=1}^k \left\| x_i^j - c_j \right\|^2, \quad (20)$$

where $\left\| x_i^j - c_j \right\|^2$ is a gap within a feature position and the centre c_j with identical groups and specify an opening of n attribute location and of alike clusters centres.

4.4. CNN

CNNs consist of layers viz. input, convolutional, pooling, and fully connected. Input layer being the first layer that takes raw data and encode it into channels and a batch of a specified size. Convolutional layers extract attributes from previous layer to next layer. Mathematically this layer can be depicted as below:

$$y = X * W \rightarrow Y[i, j] = \sum_{k1=-\infty}^{+\infty} \cdot \sum_{k2=-\infty}^{+\infty} X[i - k1, j - k2] W[k1, k2], \quad (21)$$

where X is a 2D input and W filter matrix. A Rectified Linear Unit layer (ReLU) assigns nought to minus quantity. ReLU activates the output of the preceding layer, and its function is $f(x) = \max(0, x)$. This output becomes the input of a pooling layer to reduce calculations quantity (down sampling). Lastly, the fully connected layers that calculate the output scores, and final feature map classification task. Figure. 5 depicts CNNs structure.

5. Conclusion

In this paper a short background of a MG system and its protection challenges due to symmetric and asymmetric faults is explained in detail. Fault detection and localization techniques are

evaluated. Conventional protection devices that detect, protect the MG system and their limits are reviewed. Due to conventional devices limits in detecting and localizing faults in AC-DC MG systems ML methods are reviewed. More emphasis on PCA, CNN, GA, K-means, and XAI algorithms was conferred due to their capabilities of classifying, detecting and localizing faults and moreover big data handling.

Acknowledgements

This work was supported in part by the South African National Research Foundation (Grant Nos. JCR230704126719 and 137951) and the South African Eskom Tertiary Education Support Programme.

References

- [1] Y.-Y. Hong, M. T. A. M. Cabatac, Fault detection, classification, and location by static switch in microgrids using wavelet transform and taguchi-based artificial neural network, *IEEE systems journal* 14 (2019) 2725–2735.
- [2] B. K. Panigrahi, P. K. Ray, P. K. Rout, S. K. Sahu, Detection and location of fault in a micro grid using wavelet transform, in: 2017 International Conference on Circuit, Power and Computing Technologies (ICCPCT), IEEE, 2017, pp. 1–5.
- [3] S. Sairam, S. Seshadhri, G. Marafioti, S. Srinivasan, G. Mathisen, K. Bekiroglu, Edge-based explainable fault detection systems for photovoltaic panels on edge nodes, *Renewable Energy* 185 (2022) 1425–1440.
- [4] Y. Seyedi, H. Karimi, S. Grijalva, J. Mahseredjian, B. Sanso, A supervised learning approach for centralized fault localization in smart microgrids, *IEEE Systems Journal* 16 (2021) 4060–4070.
- [5] R. Pradhan, P. Jena, An innovative fault direction estimation technique for ac microgrid, *Electric Power Systems Research* 215 (2023) 108997.
- [6] A. Srivastava, A. Kumar, A. Kumar, S. Sriharsh, S. Parida, H. Priyadarshi, Random forest based fault detection and localization in microgrid using simplified measurements, in: 2023 IEEE IAS Global Conference on Emerging Technologies (GlobConET), IEEE, 2023, pp. 1–6.
- [7] L. Zhang, N. Tai, W. Huang, J. Liu, Y. Wang, A review on protection of dc microgrids, *Journal of Modern Power Systems and Clean Energy* 6 (2018) 1113–1127.
- [8] S. Admasie, S. B. A. Bukhari, T. Gush, R. Haider, C. H. Kim, Intelligent islanding detection of multi-distributed generation using artificial neural network based on intrinsic mode function feature, *Journal of Modern Power Systems and Clean Energy* 8 (2020) 511–520.
- [9] Y. Seyedi, H. Karimi, S. Grijalva, J. Mahseredjian, B. Sanso, A supervised learning approach for centralized fault localization in smart microgrids, *IEEE Systems Journal* 16 (2021) 4060–4070.
- [10] J. Hu, A. Lanzon, Distributed finite-time consensus control for heterogeneous battery energy storage systems in droop-controlled microgrids, *IEEE Transactions on smart grid* 10 (2018) 4751–4761.

- [11] Q. Wan, S. Zheng, C. Shi, A rapid diagnosis technology of short circuit fault in dc microgrid, *International Journal of Electrical Power & Energy Systems* 147 (2023) 108878.
- [12] K. Faraoun, A. Boukelif, Neural networks learning improvement using the k-means clustering algorithm to detect network intrusions, *INFOCOMP Journal of Computer Science* 5 (2006) 28–36.
- [13] V. H. Phung, E. J. Rhee, A high-accuracy model average ensemble of convolutional neural networks for classification of cloud image patches on small datasets, *Applied Sciences* 9 (2019) 4500.